INTL JOURNAL OF ELECTRONICS AND TELECOMMUNICATIONS, 2024, VOL. 70, NO. 4, PP. 831-838
Manuscript received August 24, 2024; revised October 2024. doi: 10.24425/ijet.2024.152067

Suitability of acoustic power amplifiers as power amplifiers in underwater communication systems

Aleksander M. Schmidt, Jan H. Schmidt, and Iwona Kochańska

Abstract—The paper presents selected acoustic power amplifiers from among those currently available. The results of a series of measurements characterising the amplifiers are presented. The measured amplitude and phase characteristics as a function of frequency for four selected amplifiers are analysed. The spectra of the output signal in the band from 4 kHz to 30 kHz are presented. The usefulness of the selected amplifiers in an underwater communication system is assessed.

***Keywords*—power amplifier; transmitter; underwater communication; amplitude; phase; spectrum**

I. Introduction

DUE to the attenuation of radio waves underwater, ultrasound technology is used increasingly broadly in this environment [1]-[3]. Systems that provide communication in both a simple configuration, i.e. a single user with another user, and in a more complex structure, such as a user exchanging information with other users within a network of devices, are particularly desirable. The needs are large and are used in the currently strongly developing energy and oil industries, but also in fishing and military applications. Such systems are often used to control devices located under the water surface. In such devices, one of the main components is a power amplifier, which is one of the components in the transmission path. Its task is to amplify the generated signal to the level of voltage value, and therefore electrical power, making it possible for the connected transducer to generate an acoustic wave with the desired parameters.

The article presents tests of amplifiers in order to assess the possibilities of their use in the considered underwater communication system. The outputs of acoustic power amplifiers have a low output impedance. They are ready for use with loads typically between 2 and 8 Ohms, while the electrical impedance of hydroacoustic transducers typically ranges between the single hundreds and the single thousands of Ohms. This requires the use of matching circuits of the amplifier output impedance to the impedance of hydroacoustic transducers in the transmission paths of the systems. [4]-[7].

Due to the fact that in this article the authors limit themselves to assessing the suitability of the tested power amplifiers for underwater communication systems. Therefore, only measurements of electrical parameters of signals at the amplifier output were performed and hydroacoustic parameters were not measured, which is a separate research issue. The studies were conducted for resistive loads and optimal values for the tested amplifiers.

II. Selection of power amplifiers

Existing and developing underwater acoustic communication systems use narrowband and broadband signals. In order to send a signals through the underwater channel, the signal representing the symbol is converted into a form that is resistant to the phenomena occurring in the channel. This is accomplished using an appropriate modulation technique. Typically, coherent modulations are used for transmission in the less demanding vertical channel to realize high-speed data transmission, and incoherent modulations in the horizontal channel. Both modulations occur with a single carrier frequency or multiple carrier frequencies. Many communication systems are based on various types of spread spectrum techniques such as chirp spread spectrum (CSS), direct sequence spread spectrum (DSSS), and frequency-hopping spread spectrum (FHSS). Other efficient communication systems use the orthogonal frequency division multiplexing (OFDM) technique. [8]-[13]

Modern power amplifiers operate in class D. This is an architecture characterised by a high efficiency of around 90%. They are distinguished by much lower losses compared to earlier designs of class A, B and AB power amplifiers. Their operating principle is based on the well-known pulse width modulation (PWM). The key advantage of using PWM is efficiency. Since the amplifier transistors are either fully on or fully off, they are only in an intermediate state for a brief time, during which the greatest energy losses occur. These features allow for a compact design. For the above-mentioned reasons, the focus was on the selection of amplifiers operating in class D.

Table I lists selected amplifiers, which differ in the range of supply voltage values, minimum load resistance value and output power. The voltage range is between 10 V for the

This paper shows the results of research conducted within the project No. DOB-SZAFIR/01/B/017/04/2021 financed by The National Centre for Research and Development

Aleksander M. Schmidt, Jan H. Schmidt and Iwona Kochańska are affiliated with the Gdańsk University of Technology, Poland (e-mail: aleksander.schmidt@pg.edu.pl, jan.schmidt@pg.edu.pl, iwona.kochanska@pg.edu.pl)

TPA 3223 and 53 V for the TPA 3255. The minimum and maximum supply values mean that, for example, the TPA 3250 amplifier can be supplied with a voltage from a minimum value of 12 V to a maximum value of 36 V. However, the supply value affects the value of the output power. For lower supply voltages, we will obtain a lower value of the output power. The

TABLE I
SELECTED POWER AMPLIFIERS

Parameters	Amplifier			
Name	TPA 3250	TPA 3251	TPA 3223	TPA 3255
Architecture	Class-D	Class-D	Class-D	Class-D
Power Supply (max/min) [V]	36/12	36/12	42/10	53/18
Load (min) [Ω]	1.5	1.5	1	2
Output power (mono/stereo)	130/70	350/175	400/200	600/300

output power values given in the table are only possible when the system is powered at the maximum value. The TPA 3255 amplifier has the largest range of supply values and output powers. The TPA 3223 amplifier has the lowest load value, i.e. 1 Ω. Two of them, the TPA 3250 and TPA 3251, can be loaded with a minimum resistance of 1.5 Ω. On the other hand, the amplifier with the highest output power can be loaded with a minimum impedance of 2 Ω.

All the tested power amplifier starter kits can operate in three output configurations. The first configuration assumes independent four-channel operation, as shown in Fig. 1a. The second structure shown in Fig. 1b assumes independent two-channel operation. In this arrangement, the first load should be connected in series between output A and output B, and the second load between output C and D. In this case, the output voltage is doubled compared to the four-channel setting. The third arrangement shown in Fig. 1c assumes the operation of the power amplifier with a single load. In this case, the two output channels are paralleled. That is, output A is connected to output C and output B is connected to output D. The single load is connected in series between outputs A and C and outputs B and D. Such a connection of the load to the amplifier module doubles the output current of the power amplifier compared to the first and second configurations while simultaneously doubling the voltage.

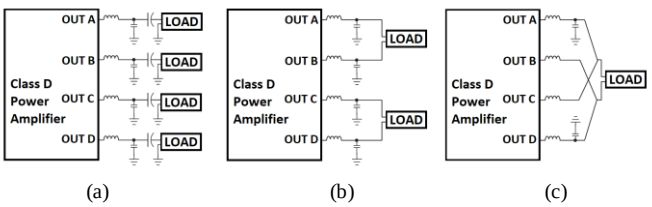

Fig. 1. Output configurations of the selected power amplifiers (a) 4 channel-single-ended (b) 2 channel-bridge-tied load (c) 1 channel-parallel bridge-tied

III. INFRASTRUCTURE OF MEASURING STATION

The block diagram below (Fig. 2) presents the measurement system used to perform all measurements necessary to plot the characteristics presented in the article.

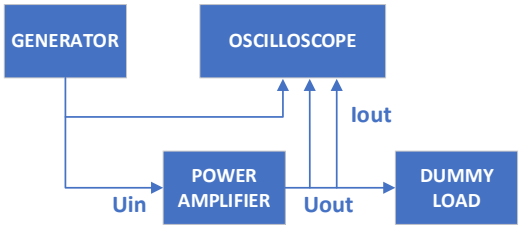

Fig. 2. Block diagram of the measuring station

In the photo (Fig. 3), we can see the equipment used during the measurements. These are two power supplies with output parameters of 30 V and 5 A. They were connected in series to obtain a supply voltage of 48 V. A function generator generated the test signals, with a 10% duty cycle and a continuous signal. These signals were fed to the power amplifier evaluation boards and were simultaneously measured using an oscilloscope. The measurement of the voltage of the amplified output signal was performed using a differential probe, while the measurement of the output current was performed using a current probe. Three power resistors with values of 2.2 Ω, 3.9 Ω, and 4.7 Ω were used as the load.

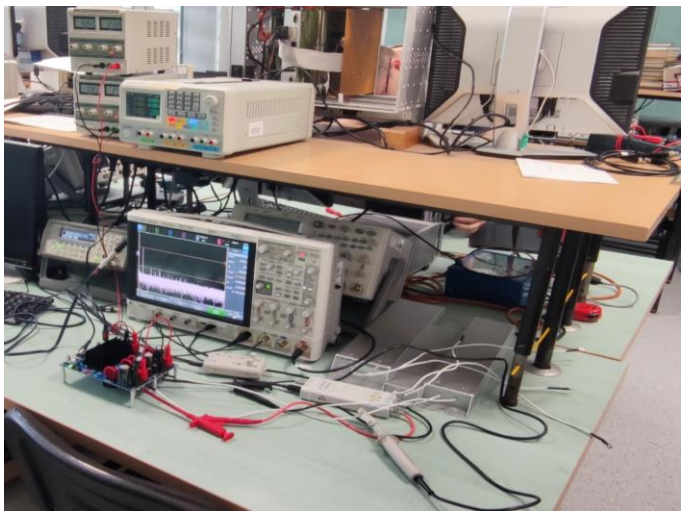

Fig. 3. Infrastructure of the measuring station

IV. MEASURED PARAMETERS

In order to determine the suitability of the selected power amplifiers, four evaluation modules with the selected TPA 3250, TPA 3251, TPA 3223, TPA 3255 amplifier circuits installed were tested. For this purpose, four types of characteristics were measured. The basic characteristic is the response of the evaluation board circuit to excitation with a signal with given amplitudes in the range from approx. 100 mVpp to approx. 3.5 Vpp. These characteristics provide information about the output power that can be obtained with a specific input signal amplitude at the specific load value. The amplitude characteristics of the amplifier circuits were measured as a function of frequency. The value of the amplifier output amplitude should not depend on the frequency and should be constant over the entire usable range of the frequency band, assuming that the input signal amplitude remains constant. This condition is quite difficult to meet for most power amplifiers and in practice linear changes in amplitude are accepted. The third in order are phase characteristics as a function of frequency. All the above characteristics were

measured for three loads with values of 2.2 Ω, 3.9 Ω and 4.7 Ω. The signal spectrum was also checked in the band of the expected use of the underwater communication system, i.e. from 4 kHz to 30 kHz. Spectrum verifications were performed for continuous operation and with a duty cycle of 10%.

In order to assess the occurrence of additional components at the amplifier output with frequencies that are an integer multiple of the input signal frequency, the total harmonic distortion (*THD*) was calculated for continuous operation and operation with a 10% duty cycle in accordance with formula (1). U_n means the RMS values of the harmonics of the measured output signal, while U_1 is the RMS value of the fundamental frequency. The summing took into account the first 5 harmonics (M=5). The calculations were made for signals generated at the edges of the assumed transmission bands.

$$THD = 100 \cdot \sqrt{\sum_{n=2}^{M} \left(\frac{U_n}{U_1}\right)^2} \ [\%] \qquad (1)$$

V. Measurements Results

Figure 4a, Fig. 4b, and Fig 4c show graphs of the output power values of the selected amplifiers as a function of the input signal amplitude expressed in Vpp. Figure 4a shows the results obtained by loading the output of each of the amplifier development kits with a resistance of 2.2 Ω. The graph shows that the highest output power was obtained for the TPA 3255 amplifier and the lowest output power was obtained for the TPA 3223, but it has the largest range of input signal values, which translates into an increase in the resolution of the output power settings.

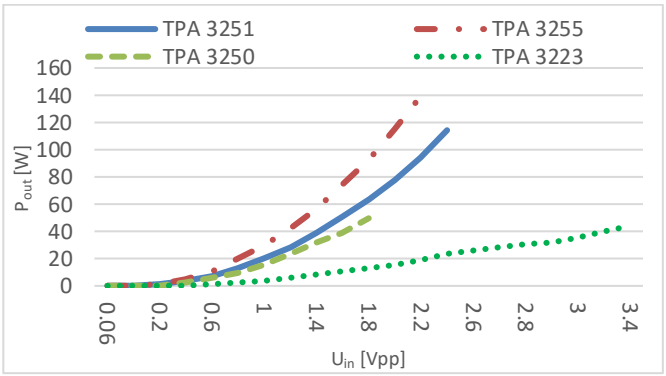

(a)

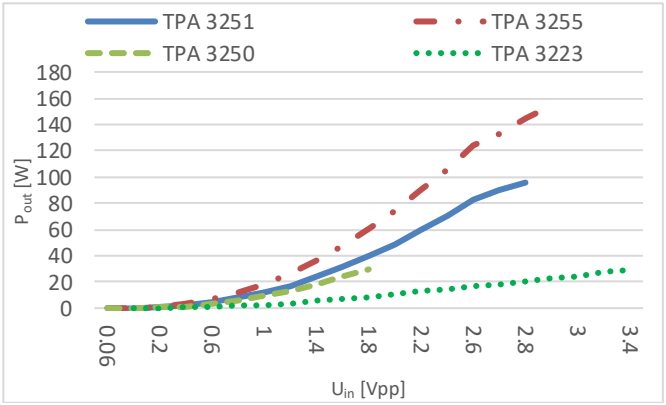

(b)

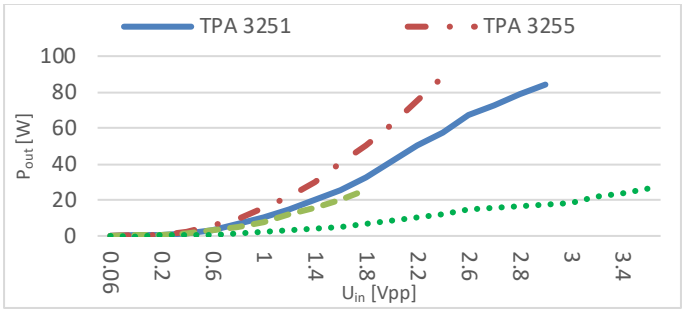

(c)

Fig. 4. Output power of the power amplifiers for (a) 2.2 Ω (b) 3.9 Ω (c) 4.7 Ω load

Figure 4b shows the output power measurements after loading the amplifying circuits with a resistance of 3.9 Ω. In this case, we see a slight increase in the range of the input signal values for the TPA 3255 and TPA 3251. Such an increase in the input signal amplitude range had a positive effect on increasing the resolution of the output power settings. For the TPA 3255 with a 3.9 Ω load, we also see a slight increase in the output power. In Fig. 4c we can see the measurement results for the highest value of the load resistance of the amplifier system, i.e. 4.7 Ω. In accordance with the assumptions, with the increase in the load impedance value, the value of the output power for each of the amplifiers decreased.

In Fig. 5a, Fig 5b, Fig. 5c, and Fig. 5d, the characteristics of the output power as a function of the input signal amplitude value for three different load values are presented for each power amplifier separately. These graphs show which load value is the most advantageous in terms of output power and the input signal amplitude range. These graphs show the agreement of the measurements with the theory. For a lower load impedance value, a higher output power value is obtained. The exception is the TPA 3255 amplifier, whose results are presented in Fig. 5d. This amplifier achieves its maximum output power for a load of 3.9 Ω. For this load value, the amplifier also has the largest range of the input signal voltage amplitude.

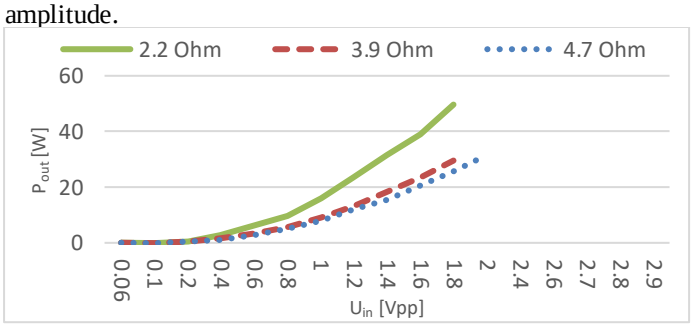

(a)

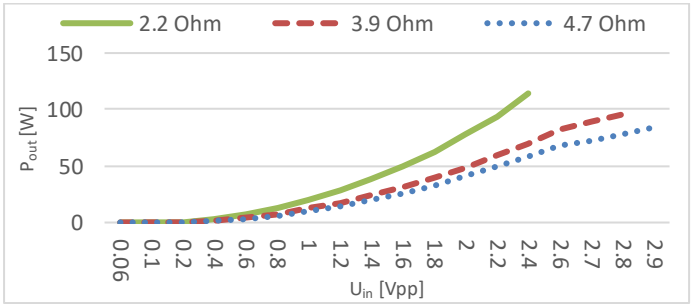

(b)

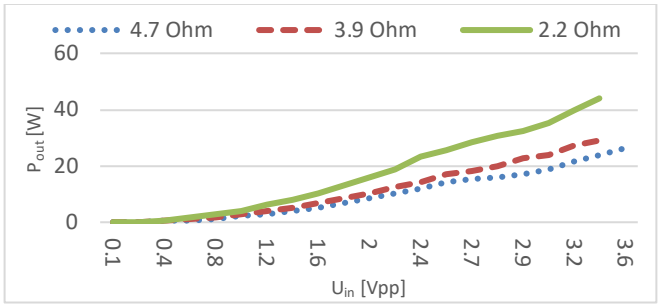

(c)

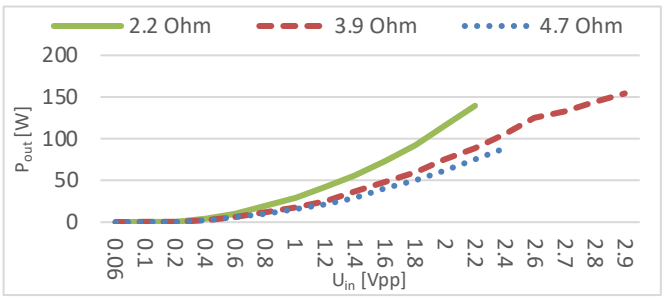

(d)

Fig. 5. Output power of the amplifiers (a) TPA 3250 (b) TPA 3251 (c) TPA 3223 (d) TPA 3255

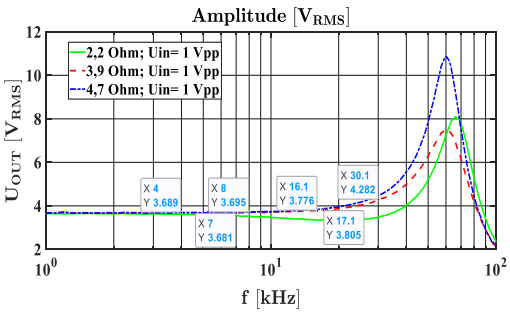

(c)

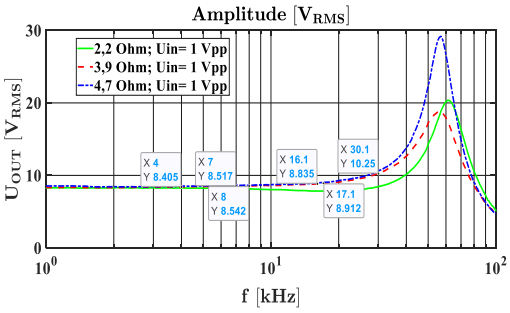

(d)

Fig. 6. Amplitude characteristic for (a) TPA 3250 (b) TPA 3251 (c) TPA 3223 (d) TPA 3255

Figure 6a, Fig. 6b, Fig6 c, and Fig. 6d, contain the amplitude characteristics of the selected amplifiers as a function of frequency from 1 kHz to 100 kHz. In the graphs, the amplitude value is expressed as the root-mean-square voltage. It can be seen that the amplitude of the output signal as a function of frequency does not change much in the tested band, i.e. from 4 kHz to 30 kHz. It is almost constant for the loads 3.9 Ω and 4.7 Ω, and only increases and then falls rapidly at around 60 kHz. The maximum value of the amplitude appears in the area of the cutoff frequency of the LC filter placed at the output of the evaluation boards module. In all cases, in the cutoff frequency area it can be seen that the highest amplitude is obtained for the load of 4.7 Ω.

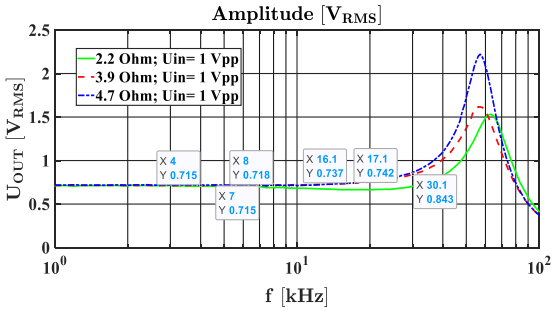

(a)

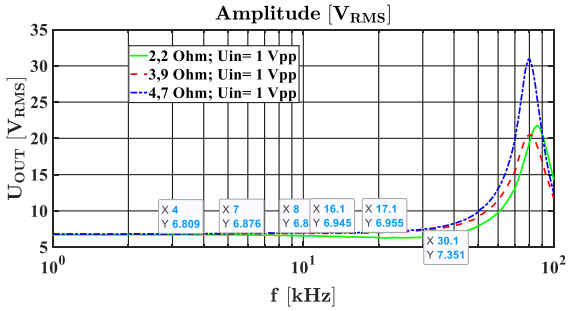

(b)

The phase characteristics are presented in Fig. 7a, Fig. 7b, Fig 7c, Fig 7d. They show the change in the phase of the output signal relative to the input signal. Our considered underwater communication system assumes operation in three bands, i.e. from 4 kHz to 8 kHz, another band from 7 kHz to 17 kHz, and the third from 16 kHz to 30 kHz. Therefore, the phase differences between the signal with the initial and final frequency of a given band are important. In Fig. 7a, we can see the plotted phase characteristics for the evaluation kit with the TPA 3250 power amplifier for three different loads. For the 3.9 Ω load, we can read that for the 4–8 kHz band, the phase difference is 3.7°, within the 7–17 kHz band, the phase difference is 9.9°, and for the third band, 16–30 kHz, it is14.1°. In the next figure (Fig. 7b), we can see the measurement results obtained for the TPA 3251. In this case, the phase difference is 3.8° for the first band, 7.2° for the second, and 9.3° for the third. From Fig. 7c, we can read the phase differences for the TPA 3223 amplifier kit. They are 3.5°; 9.2°, and 12.4° for the individual bands, respectively. Fig. 7d presents the measurements obtained for the TPA 3255 kit. We can see that for the first band, the phase difference is 4.4°, for the second, it is 10.3°, and for the third band, 15°. These are the largest differences among the tested starter kits, but this kit also has the highest output power. Despite the highest phase deviation values, these are acceptable values.

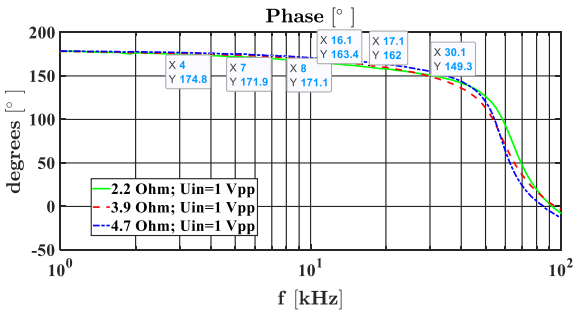

(a)

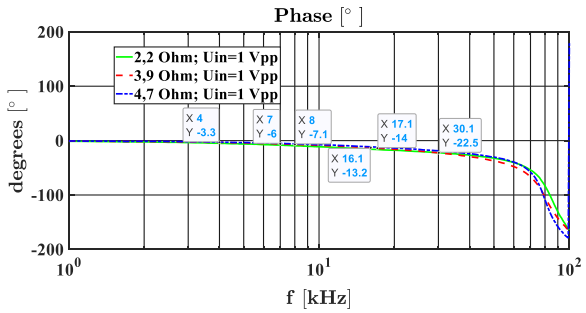

(b)

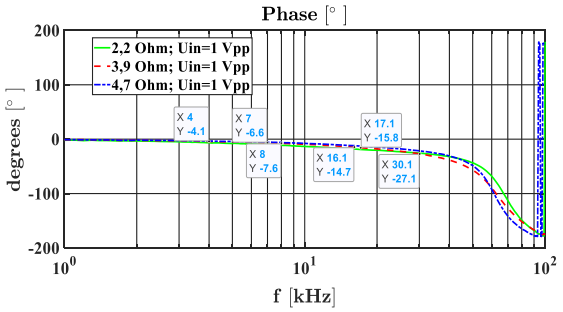

(c)

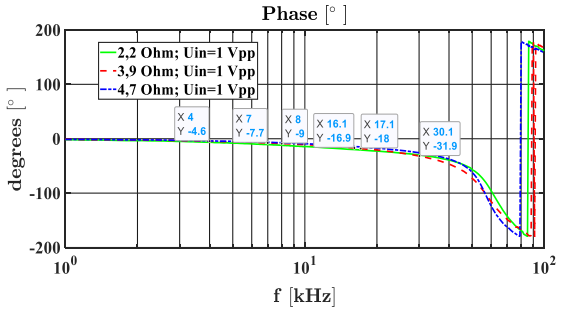

(d)

Fig. 7. Phase characteristic for (a) TPA 3250 (b) TPA 3251 (c) TPA 3223 (d) TPA 3255

All phase difference data within the three frequency bands for each development kit loaded with a 3.9 Ω, resistance are summarised in Table II.

TABLE II
PHASE DIFFERENCES IN FREQUENCY BAND FOR 3,9 Ω

Frequency band	Amplifier			
	TPA 3250	TPA 3251	TPA 3223	TPA 3255
4-8 kHz	3.7 °	3.8 °	3.5 °	4.4 °
7-17 kHz	9.9 °	7.2 °	9.2 °	10.3 °
16-30 kHz	14.1 °	9.3 °	12.4 °	15.0 °

The indicator that quantitatively and qualitatively illustrates the presence of the useful signal and other undesirable components is spectral analysis [14]. Fig. 8a, Fig. 8b, Fig. 8c, Fig. 8d, Fig. 8e, Fig. 8f present the frequency spectrum of the signal at the output of the evaluation module with the TPA 3255 amplifier loaded with the 3.9 Ω power resistor. The spectra were recorded during amplifier operation with a 10% duty cycle. That is, for 100 ms the signal from the generator was amplified, fed to the amplifier input, and for the next 900 ms the generated signal was not fed to the amplifier input. For all these cases the calculated total distortion factor *THD* was below 1%, which is a very good value.

In Fig. 8a and Fig. 8b, we can see the spectrum of signals with frequencies from the edge of the first band. Thus, in Fig. 8a, we see a spectrum in the range up to 50 kHz recorded at the output of the TPA 3255 amplifier. The difference between the amplified signal with a frequency of 4 kHz and the remaining components is 58 dB. Similarly, in Fig. 8b, we see the amplified signal with a frequency of 8 kHz and the remaining components of the spectrum. In this case, the difference is equal to 50 dB.

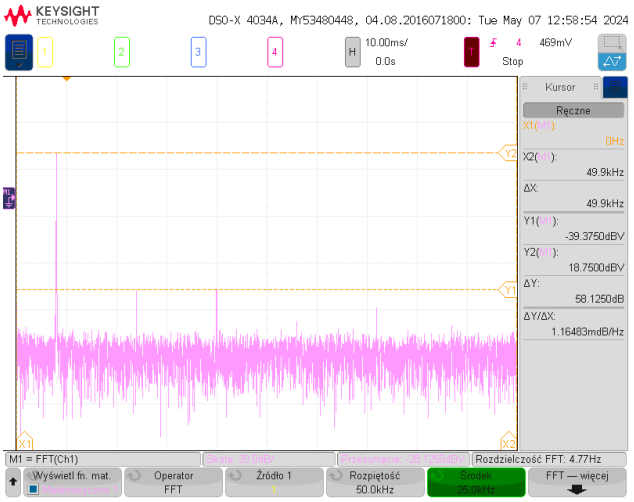

(a)

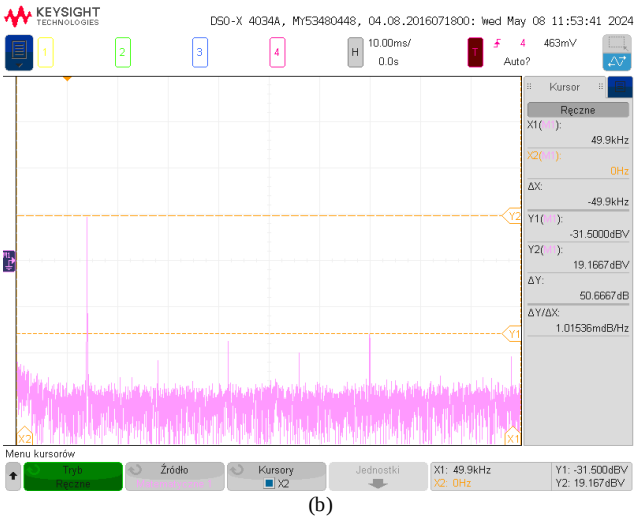

(b)

(c)

Fig. 8c shows a spectrum of a signal with a lower frequency of the second band, i.e. 7 kHz. In this case, the difference in amplitudes between the generated and amplified signal and the remaining components is 50 dB. Fig. 8d shows a spectrum of a signal with a higher frequency of the second band, i.e. 17 kHz. For such amplified signal, the difference in amplitudes is about 59 dB.

(d)

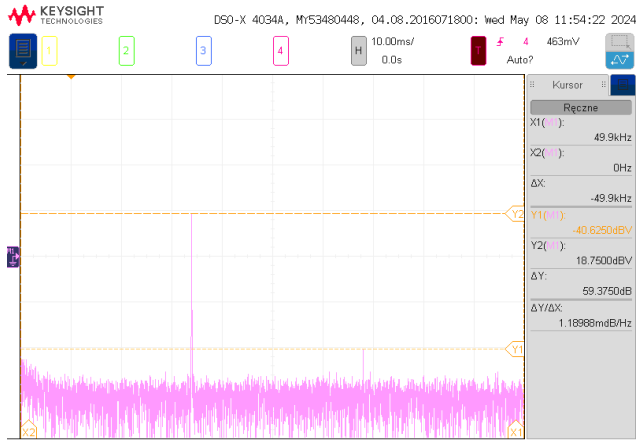

(e)

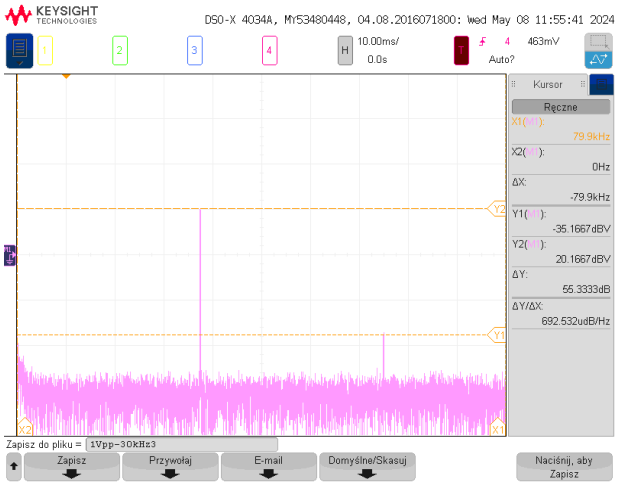

(f)

Fig. 8. Spectrum for TPA 3255 (10% duty cycle) (a) 4 kHz (b) 8 kHz (c) 7 kHz (d) 17 kHz (e) 16 kHz (f) 30 kHz

For the third band in Fig. 8e, we see the spectrum with the 16 kHz signal. The difference, as before, is approx. 59 dB. For the upper frequency of the third band, the signal spectrum is presented in Fig. 8f. The difference in the level of the amplified signal to the remaining components in this case is approx. 55 dB.

Underwater communication systems often operate in conditions close to continuous operation. In order to test this mode of operation, long-term tests were performed, consisting in feeding a continuous signal from the generator to the amplifier input, while the recordings of the operating parameters at the output were performed when the amplifier radiator reached a stabilised temperature. The tests were performed without forced air flow or additional cooling. In Fig. 9a, Fig. 9b, Fig. 9c, Fig. 9d, Fig. 9e, and Fig. 9f, we can see the spectrum for continuous operation of the TPA 3255 amplifier loaded with the 3.9 Ω power resistor. For all these cases the calculated total distortion factor *THD* was below 5%, which is a sufficient result.

In the case of the first band, Fig. 9a and Fig. 9b respectively, show the spectra of signals with components at the amplifier output with a frequency of 4 kHz and 8 kHz. The distance between the amplified signals and the remaining spectrum components is approximately 51 dB and 41 dB, respectively.

For the edges of the second band, the distance between the amplified signals and the remaining spectrum components is 42 dB, as shown in Fig. 9c and 33 dB in Fig. 9d.

The measurement results of the third band are shown in Fig. 9e and Fig. 9f and the numerical results are approximately 35 dB and approximately 58 dB, respectively. These values are clearly lower compared to the operation with a 10% duty cycle, but still acceptable [15],[16].

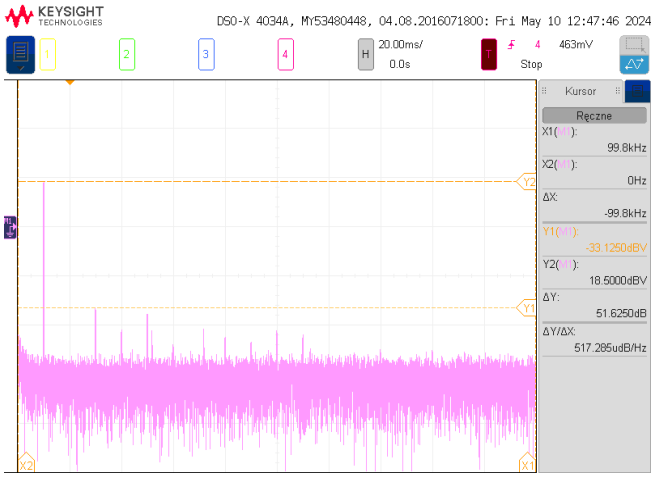

(a)

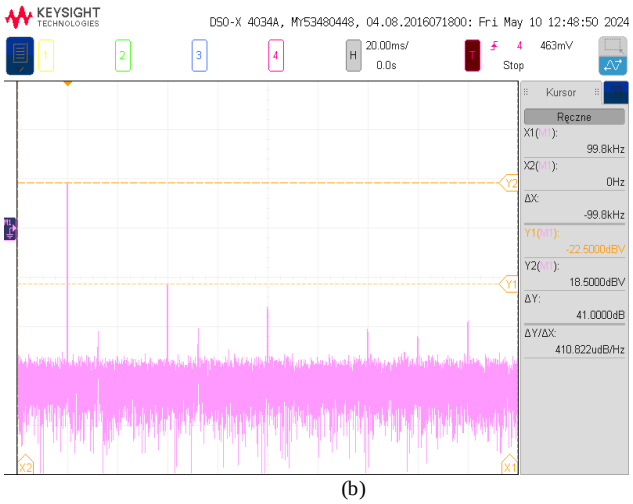

(b)

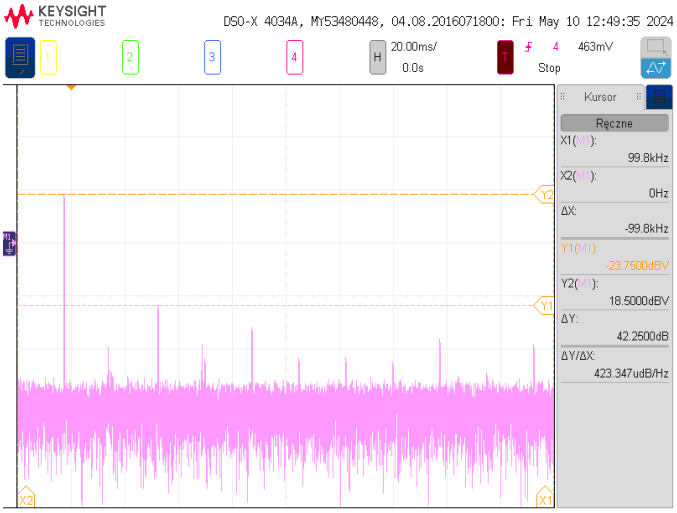

(c)

(d)

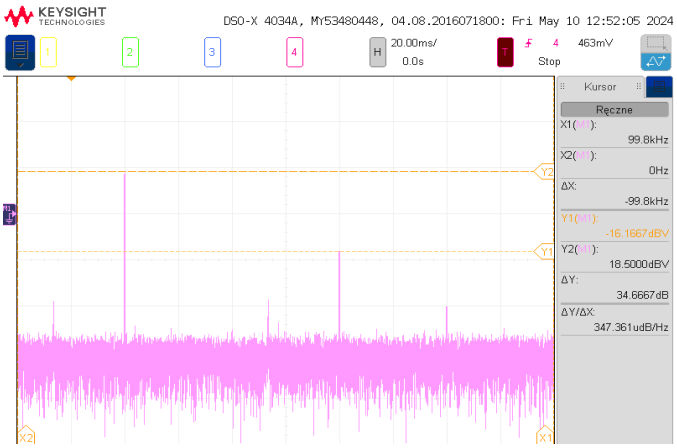

(e)

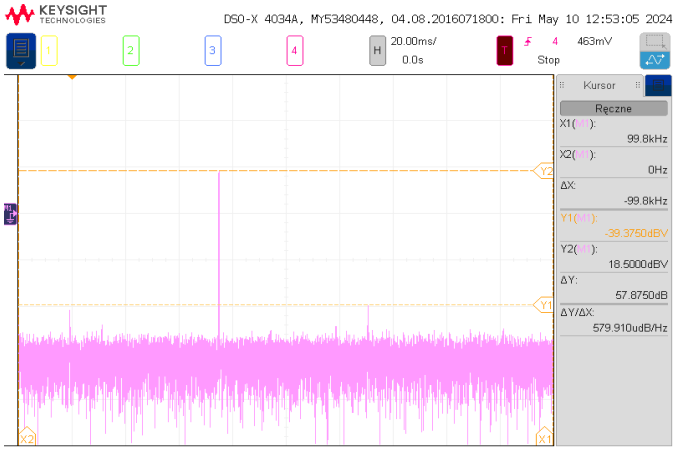

(f)

Fig. 9 Spectrum for TPA 3255 (continuous work) (a) 4 kHz (b) 8 kHz (c) 7 kHz (d) 17 kHz (e) 16 kHz (f) 30 kHz

CONCLUSION

The paper presents a series of analyses performed on commercially available evaluation modules that can be used as ready-made power amplifiers for an underwater communication system. Based on the presented measurement results, the most suitable device for a given application can be selected, depending on whether it is a system focused on energy saving or on achieving long ranges, i.e. with high output power. The TPA 3255 amplifier seems to be a compromise, as it combines both of these features. That is, it can operate in systems focused on battery operation, thanks to its broad range of supply voltages. At the same time, it is suitable for applications where the highest possible output power is required. It has an appropriate resolution of output power settings and is characterised by a linear, almost flat amplitude characteristic as a function of frequency in the range up to 30 kHz. The phase characteristic is almost linear in the tested frequency range. The difference between the amplified signal and the remaining spectrum components is between 30 and 50 dB, depending on the signal filling time. The calculated *THD* values below 1% and below 5%, respectively, for a signal with a 10% duty cycle and for a continuous signal are sufficient results. In addition, the tested sets have features usually found in mature solutions that protect against thermal and short-circuit damage. Another important aspect is the ability to easily adapt the module to ensure smooth regulation of the output power by changing the amplitude of the input signal in a controlled manner.

ACKNOWLEDGEMENTS

The research presented in the article was carried out as part of the project 'Underwater wireless communication system for unmanned and autonomous offshore platforms'.
The program No. DOB-SZAFIR/01/B/017/04/2021 is financed by The National Centre for Research and Development.

REFERENCES

[1] X. Lurton, "An introduction to underwater acoustics: Principles and applications", Springer, Berlin, 2010. ISBN-13: 978-3-540-78480-7

[2] R. J. Urick, "Principles of underwater sound for engineers", McGraw, 1983. ISBN-13: 978-0932146625

[3] P. C. Etter, "Underwater acoustic modelling and simulation", CRC Press, 2018. ISBN-13: 978-1138054929

[4] B. Cordell, "Designing audio power amplifiers" Routledge, 2nd ed., Routledge, June 13 2019. ISBN-13: 978-1138555440

[5] D. Self, "Audio power amplifier design Handbook" Routledge, 5th ed., Routledge, July 31 2009. ISBN-13: 978-0240521626

[6] J. L. Butler, C. H. Sherman, "Transducers and arrays for underwater sound", Springer, 2016, https://doi.org/10.1007/978-3-319-39044-4

[7] J. C. Cochran, "Introduction to sonar transducer design", Wiley, June 2022, ISBN-13: 978-1-119-85107-3

[8] H. S. Dol, P. Casari, T van der Zwan, R. Otnes, "Software-Defined Underwater Acoustic Modems: Historical Review and the NILUS Approach," IEEE Journal of Oceanic Engineering, vol. 42, pp. 722- 737, July 2017. https://doi.org/10.1109/JOE.2016.2598412

[9] J.H. Schmidt, A.M. Schmidt, "Underwater Acoustic Communication System Using Broadband Signal with Hyperbolically Modulated Frequency", Vibrations in Physical Systems 2021, 32(1):2021116. https://doi.org/10.21008/j.0860-6897.2021.1.16

[10] J.H. Schmidt, "Using Fast Frequency Hopping Technique to Improve Reliability of Underwater Communication System," Applied Sciences 2020, 10, no. 3: 1172. https://doi.org/10.3390/app10031172

[11] J. Schmidt, I. Kochańska, A. Schmidt, "Performance of the Direct Sequence Spread Spectrum Underwater Acoustic Communication System with Differential Detection in Strong Multipath Propagation Conditions," Archives of Acoustics, vol. 49, no. 1, pp. 129-140, 2024, https://doi.org/10.24425/aoa.2024.148771

[12] S. Zhou, Z Wang, "OFDM for Underwater Acoustic Communications", John Wiley & Sons Ltd.: Chichester, UK, 2014.

[13] I. Kochańska, J.H. Schmidt, J. Marszal, "Shallow Water Experiment of OFDM Underwater Acoustic Communications," Archives of Acoustics, vol. 54, no. 1, pp. 11-18, 2020, https://doi.org/10.24425/aoa.2019.129737

[14] A. Lewandowski, R. Matyszkiel, P. Kaniewski, „The demonstrator of power amplifier in high voltage technology", Elektronika, vol. 56, no. 2, pp. 69-71, 2015. https://doi.org/10.15199/13.2015.2.16

[15] J. Modzelewski, A. Bartosik, „Class –AB wide-band transformer power amplifiers for HF and VHF band, Elektronika, vol. 56, no. 7, pp. 52-58, 2015. https://doi.org/10.15199/13.2015.7.11

[16] M. Mikołajewski, „An analysis of a transformer Class E amplifier", Elektronika, vol. 56, no. 9, pp. 12-15, 2015. https://doi.org/10.15199/13.2015.9.2